

THE SUPERNOVA CHANNEL OF SUPER-AGB STARS

A.J.T. POELARENDS^{1,2}, F. HERWIG^{3,2}, N. LANGER¹, AND A. HEGER^{2,4,5}

Draft version October 22, 2018

ABSTRACT

We study the late evolution of solar metallicity stars in the transition region between white dwarf formation and core collapse. This includes the super-asymptotic giant branch (super-AGB, SAGB) stars, which have massive enough cores to ignite carbon burning and form an oxygen-neon (ONe) core. The most massive SAGB stars have cores that may grow to the Chandrasekhar mass because of continued shell-burning. Their cores collapse, triggering a so called electron capture supernovae (ECSN).

From stellar evolution models we find that the initial mass range for SAGB evolution is 7.5...9.25 M_{\odot} . We perform calculations with three different stellar evolution codes to investigate the sensitivity of this mass range to some of the uncertainties in current stellar models. The mass range significantly depends on the treatment of semiconvective mixing and convective overshooting. To consider the effect of a large number of thermal pulses, as expected in SAGB stars, we construct synthetic SAGB models that include a semi-analytical treatment of dredge-up, hot-bottom burning, and thermal pulse properties. To calibrate the time-dependent synthetic model, we have calibrated a number of SAGB stellar evolution models. This synthetic model enables us to compute the evolution of the main properties of SAGB stars from the onset of thermal pulses until the core reaches the Chandrasekhar mass or is uncovered by the stellar wind. Thereby, we determine the stellar initial mass ranges that produce ONe-white dwarfs and electron-capture supernovae. The latter is found to be 9.0...9.25 M_{\odot} for our fiducial model, implying that electron-capture supernovae would constitute about 4% of all supernovae in the local universe. Our synthetic approach allows us to explore the uncertainty of this number imposed by uncertainties in the third dredge-up efficiency and AGB mass loss rate. We find that for both processes, the most optimistic approach leads to about a doubling of the number of electron-capture supernovae, which provides a firm upper limit to their contribution to all supernovae of $\sim 20\%$.

Subject headings: stars: AGB and post-AGB — stars: evolution — supernovae: general — stars: neutron

1. INTRODUCTION

It is well known that, for a given initial chemical composition, it is the initial stellar mass which essentially determines the final fate of a star: lower masses produce white dwarfs, higher masses neutron stars and supernovae. The late evolution phases of stars in the transition region between white dwarfs and neutron stars is numerically difficult to model, and the relevant physics is not yet fully understood. This mass range is therefore often omitted in stellar evolution calculations. This is unsatisfactory because the uncertain initial mass region for this evolution is 7 to 12 M_{\odot} , implying that as much as half of all supernovae may originate from this transition region.

Of particular interest in this context is the evolution of so called super-asymptotic giant branch (SAGB)

stars, which ignite carbon non-explosively, but also undergo thermal pulses (Ritossa et al. 1996; Iben et al. 1997; Garcia-Berro et al. 1997; Ritossa et al. 1999; Siess 2006). These stars may end their lives either as massive ONe-white dwarfs (Nomoto 1984), or as electron capture supernovae (ECSNe), where the core collapse is triggered by electron captures before Ne ignition (Wheeler et al. 1998; Wanajo et al. 2003). Stars of larger initial mass ignite hydrostatic neon burning, form an iron core, and lead to classical core collapse supernovae (CCSNe).

The upper mass limit of SAGB stars is affected by the second dredge-up, which may occur after core He-exhaustion, and which drastically reduces the mass of the helium core. At this point and throughout the following early SAGB phase carbon burning transforms the CO core into an ONe core (Nomoto 1987; Ritossa et al. 1996; Iben et al. 1997; Garcia-Berro et al. 1997; Ritossa et al. 1999). Since the temperature is not high enough to ignite Ne, the core cools, electron degeneracy in the core increases, and the structure of the SAGB star outside of the ONe-core is very similar to the most massive CO-core AGB stars (Frost et al. 1998, for a general review of AGB evolution see Iben & Renzini 1983; Habing 1996 and Herwig 2005). The degenerate core is surrounded by the He- and H-shell sources, which eventually produce thermal pulses due to the instability of the helium shell source (Yoon et al. 2004).

In this situation, the mass of the H-free core contin-

¹ Astronomical Institute, P.O. Box 80000, NL-3508 TA Utrecht, The Netherlands, a.j.t.poelarends@astro.uu.nl, n.langer@astro.uu.nl

² Theoretical Astrophysics Group, T-6, MS B227, Los Alamos National Laboratory, Los Alamos, NM 87545, USA, aheger@lanl.gov

³ Keele Astrophysics Group, School of Physical and Geographical Sciences, Keele University, Staffordshire, UK, fherwig@astro.keele.ac.uk

⁴ Department of Astronomy and Astrophysics, University of California, Santa Cruz, CA 95064, USA

⁵ Department of Astronomy and Astrophysics, University of Chicago, 5640 S. Ellis Avenue, Chicago, IL 60637, USA

ues to grow. If the core mass reaches the Chandrasekhar mass of $1.375 M_{\odot}$, the core will collapse triggered by electron captures on ^{24}Mg and ^{20}Ne , and the star will become an ECSN (Miyaji et al. 1980; Miyaji & Nomoto 1987; Hashimoto et al. 1993). Recent studies by Ritossa et al. (1996); Garcia-Berro et al. (1997); Iben et al. (1997); Ritossa et al. (1999) and Siess (2006) have shown that the mass fraction of ^{24}Mg in the ONe-core is smaller than previously thought, which diminishes the role of electron captures on ^{24}Mg . While Gutiérrez et al. (2005) found that unburnt carbon in the degenerate ONe core could trigger an explosion at densities of $\sim 10^9 \text{g cm}^{-3}$, we disregard this possibility furtheron since its observational implications are not worked out, and therefore this scenario can not yet be confronted with supernova observations.

The initial mass range for core collapse after SAGB evolution depends on the effective core growth and mass loss of the SAGB star. Larger mass loss rates lead to a shorter duration of the SAGB phase. For very high SAGB mass loss, there is no time for any significant core growth, and the initial mass range for ECSNe will be very small. On the other hand, the core growth rate in SAGB stars depends on the the hydrogen shell burning and thus on two crucial factors, hot-bottom burning (Sackmann & Boothroyd 1991; Ventura et al. 2005), and the efficiency of the third dredge-up.

Previous studies of SAGB stars have concentrated on the evolution of the stellar cores (Nomoto 1984, 1987). According to these models, stars with helium cores between 2.0 and $2.5 M_{\odot}$ form ONe cores and explode as ECSN, leaving a neutron star less massive than $1.3 M_{\odot}$. Ritossa et al. (1996, 1999), Iben et al. (1997) and Garcia-Berro et al. (1997) studied the evolution of complete SAGB stellar models in detail. They describe SAGB thermal pulses, and an outward mixing event which they called dredge-out, in which the convective envelope connects to a convection zone on top of the helium burning layer. Siess (2006), who studied the effects of the carbon flame and of thermonuclear reactions on the structure of the ONe core, finds similar results.

Thermal pulses in AGB evolutionary models require high numerical resolution, both in time and space. The interpulse period decreases with increasing core mass to eventually only a few years for the most massive AGB star. In order to follow the evolution of SAGB stars with very high core masses, orders of magnitude more thermal pulses (up to 10000s) have to be computed compared to low-mass AGB stars, which experience only tens of thermal pulses. For this reason, no detailed stellar evolution calculations through the entire super-TP-AGB phase exist. Ritossa et al. (1999) attempted to characterize stars that would end as ECSN. Based on the assumption of a constant SAGB mass loss rate of $10^{-4} M_{\odot}/\text{yr}$, they speculated that out of their set of four calculated models (9, 10, 10.5 and $11 M_{\odot}$) only the $11 M_{\odot}$ model would explode as an ECSN. The other models would lose all their envelope before the core has grown enough, and their final fate would be an ONe white dwarf. Eldridge & Tout (2004b) determine a minimum mass for supernova explosion around $7 M_{\odot}$ (with overshooting), or around $9 M_{\odot}$ (without overshooting), again without being able to calculate the stellar evolution models through the final phases.

Models of SAGB evolution suffer from two dominant sources of uncertainty: mass loss and the efficiency of the third dredge-up. To explore these uncertainties would require to compute several model grids, which is not feasible at this time. We therefore take a different approach and use the fact that TP-AGB stars, after a brief transition phase, reach a quasi-steady state in which the important structural quantities evolve in a simple and predictable way as function of time. This approach of synthetic AGB modeling has already been successfully used for low-mass and massive AGB stars (Renzini & Voli 1981; Iben & Renzini 1983; Marigo et al. 1996).

In the following, we first describe the detailed stellar evolution models (Sect. 2) and identify the initial mass range for SAGB stars by calculating the pre-AGB evolution phase up to the end of the second dredge-up and possibly C-ignition, using three different stellar evolution codes (Sect. 3). Next, we describe our SAGB stellar evolution models (Sect. 4), and our synthetic SAGB evolution model (Sect. 5). We present our results in Sect. 6 and concluding remarks in Sect. 7.

2. NUMERICAL METHODS

We use three different stellar evolution codes to calculate the evolution of solar metallicity stars up to the end of the second dredge-up, or to Ne-ignition. We used the codes STERN (Langer 1998; Heger et al. 2000), EVOL (Blöcker 1995; Herwig 2000) and KEPLER (Weaver et al. 1978; Heger et al. 2000). All three codes use the OPAL opacities (Iglesias & Rogers 1996), and are equipped with up-to-date input physics, including a nuclear network with all relevant thermonuclear reactions.

For our investigation, the most relevant difference between the codes concerns the treatment of convective and semiconvective mixing. As we will see, these affect the He-core mass after central He-burning, and thereby the final fate of the stellar model. STERN and KEPLER use the Ledoux-criterion to determine convective instability, and take semiconvection into account. In KEPLER the treatment of semiconvection leads to rather fast mixing. Specifically, it is approximated as a diffusive process with a diffusion coefficient that is 10% of the radiative diffusion coefficient. Typically, this leads to a 1000x shorter mixing time scale as for the default value of Langer et al. (1983) as used in STERN ($\alpha_{\text{sem}} = 0.01$). No modification to the temperature gradient is assumed, i.e., the radiative temperature gradient is used. Additionally, in KEPLER convection zones are extended by one extra grid point where fast mixing is assumed, to mimic convective overshooting. In the EVOL code, convective boundaries are determined by the Schwarzschild criterion, and semiconvection is not treated as a separate mixing process. Mixing beyond convective boundaries is treated by adopting an exponentially decaying diffusion coefficient (Herwig et al. 1997; Herwig 2000). Such mixing may be induced by convective overshooting (Freitag et al. 1996), or internal gravity waves (Denissenkov & Tout 2003), or a combination of both (Young et al. 2005). For the pre-AGB evolution, the overshoot parameter in EVOL has been set to $f = 0.016$, which was shown by Herwig (2000) to reproduce the observed main sequence width in the HR diagram of young open clusters. Effectively, the strength of mixing in KEPLER lies in between that of STERN (slow semiconvective mixing) and that of EVOL

TABLE 1

SUMMARY OF OUR DETAILED STELLAR EVOLUTION SEQUENCES. THE COLUMNS GIVE THE MODEL IDENTIFIER (S MEANS STERN, E IS EVOL, AND K IS KEPLER), THE INITIAL MASS (M_{\odot}), THE HELIUM CORE MASS PRIOR TO THE SECOND DREDGE-UP (M_{\odot}), THE HELIUM CORE MASS AFTER THE SECOND DREDGE-UP (M_{\odot}), INFORMATION THE END OF THE SIMULATION, AND THE FINAL FATE OF THE SEQUENCE ACCORDING TO OUR FIDUCIAL SAGB EVOLUTION PROPERTIES (MASS LOSS, DREDGE-UP, AS DESCRIBED IN SECT. 6.4)

Model	M_i	pre-2DU	post-2DU	comments	fate
S5.0	5.0	0.91	0.84	14 TP	CO WD
S8.5	8.5	1.73	1.02	10 TP	CO WD
S9	9	1.90	1.07	30 TP	ONe WD
S9.5	9.5	2.00	1.11		ONe WD
S10	10	2.14	1.16	55 TP	ONe WD
S10.5	10.5	2.30	1.20		ONe WD
S11	11	2.45	1.23		ONe WD
S11.5	11.5	2.61	1.27	15 TP	ONe WD
S12	12	2.79	1.32	dredge-out	ECSN
S12.5	12.5	2.95	2.95	dredge-out	CCSN
S13.0	13	3.13	3.13	Ne ignition	CCSN
S16.0	16	4.33	4.33	Ne ignition	CCSN
E6.5	6.5	1.59	0.99		CO WD
E7.5	7.5	1.90	1.07		ONe WD
E8.5	8.5	2.27	1.24		ONe WD
E9.5	9.5	2.65	1.43		CCSN
E10.0	10.0	2.82	2.82	dredge-out	CCSN
E10.5	10.5	3.00	3.00	Ne ignition	CCSN
E0099	9.0	2.15	1.17	$f_{\text{over}} = 0.004$	
K8	8.0	1.808	1.168		ONe WD
K8.5	8.5	1.955	1.247		ONe WD
K9	9.0	2.130	1.338		ONe WD
K9.1	9.1	2.161	1.357		ECSN
K9.2	9.2	2.190	1.548	Ne ignition	CCSN
K9.3	9.3	2.221	1.603	Ne ignition	CCSN
K9.4	9.4	2.253	1.690	Ne ignition	CCSN
K9.5	9.5	2.283	1.799	Ne ignition	CCSN
K10	10.0	2.439	2.315	Ne ignition	CCSN
K10.5	10.5	2.598	2.596	Ne ignition	CCSN
K11	11.0	2.759	2.759	Ne ignition	CCSN

(Schwarzschild criterion for convection is similar to very fast mixing in semiconvective regions).

The EVOL code has previously been used to study low-mass (e.g. Herwig & Austin 2004) and massive AGB stars (Herwig 2004a,b). KEPLER has in the past been applied to study massive stars (Woosley et al. 2002), but has not previously been used for AGB simulations. STERN has been used for low mass AGB stars (Langer et al. 1999; Herwig et al. 2003; Siess et al. 2004) as well as for massive stars (Heger et al. 2000; Heger & Langer 2000).

3. PRE-AGB EVOLUTION AND THE INITIAL MASS RANGE FOR SAGB STARS

In order to identify the processes that lead to SAGB star formation we calculate stellar evolution sequences with initial masses between $6.5 M_{\odot}$ and $13 M_{\odot}$, starting from the zero age main sequence until the completion of the second dredge-up or Ne ignition (Table ??). Up to the end of the second dredge-up, no mass loss is taken into account. The initial metallicity of our models is $Z = 0.02$. The effects of rotation or magnetic fields are not taken into account.

3.1. H- and He-core burning

The evolution of stars toward the SAGB has been studied previously (Ritossa et al. 1996; Iben et al. 1997; Garcia-Berro et al. 1997; Ritossa et al. 1999; Siess 2006),

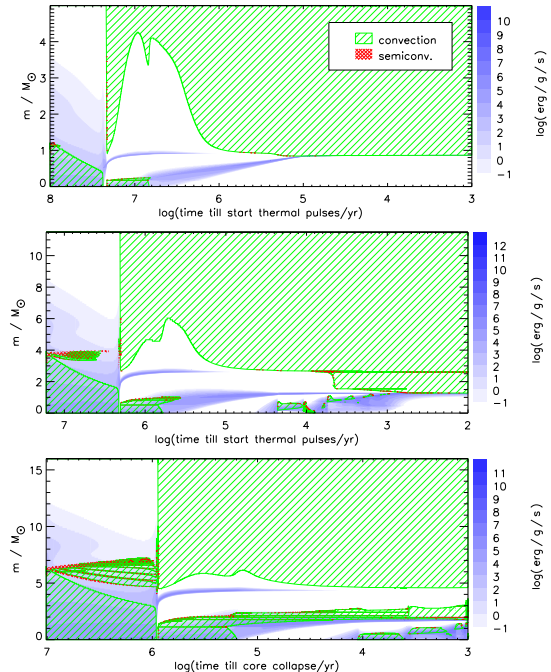


FIG. 1.— Time evolution of convection zones and energy generation for three evolution sequences with different mass, computed with STERN. The initial masses and evolution scenarios are: top panel: $5 M_{\odot}$, massive AGB, middle panel: $11.5 M_{\odot}$, SAGB, lower panel: $16.0 M_{\odot}$ star, Fe-core, CCSN. Convective regions are indicated by green hatching while semiconvective regions are indicated by red cross-hatching. The energy generation from nuclear burning is shown in greyscale with a legend to the side in units of $\log \text{erg g}^{-1} \text{s}^{-1}$.

and our simulations qualitatively confirm these results, although quantitative differences occur. In our STERN models, a consequence of including semiconvection is that during core helium burning, a semiconvective layer limits the mixing between the inner helium burning core and the outer convective core, which still grows in mass (see also Fig. 1 below). This decreases the lifetime of the core helium burning phase, because the available amount of helium is reduced, and leads to smaller helium and CO-core masses compared to models which use the Schwarzschild criterion for convection.

Girardi et al. (2000) studied the effect of convective overshooting on the maximum initial mass for which stars do not ignite carbon, M_{up} , and which defines the lower limit of SAGB stars. They find for models without overshooting a value of M_{up} of $6 M_{\odot} \dots 7 M_{\odot}$, while a moderate amount of overshooting reduces this by $1 M_{\odot}$. In our models we find $M_{\text{up}} = 7.5 M_{\odot}$ (EVOL/KEPLER), while our STERN models – without any overshooting – give $M_{\text{up}} = 9.0 M_{\odot}$. We will discuss these differences in the next paragraph.

3.2. The second dredge-up

The second dredge-up is a key difference between SAGB stars and massive stars that encounter Fe-core collapse. After core-He exhaustion, the core resumes contraction while the envelope expands. As the star evolves up the asymptotic giant branch the envelope convection deepens, and eventually penetrates into the H-free core. Only due to this mixing event is the H-free core mass sufficiently reduced so that an electron-degenerate core

can form which then cools and prevents Ne from igniting. If the core mass after the 2nd dredge-up is smaller than the Chandrasekhar mass, an electron-degenerate core will form and the He- and H-shells will eventually start the thermal pulse cycle.

The dependence of the late evolutionary phases, including the second dredge-up, on the initial mass is illustrated in the Kippenhahn-diagrams of three sequences computed with the STERN code shown in Figure 1. All models evolved through core-H and core-He burning. In the $5.0 M_{\odot}$ models, the hydrogen burning terminates, and the second dredge-up reduces the helium core mass by about $0.2 M_{\odot}$. When the helium shell source gets close to the bottom of the convective envelope, hydrogen reignites, and the thermal pulse cycle starts. For the $11.5 M_{\odot}$ model, central hydrogen and helium burning is followed by off-center carbon ignition. During the carbon burning phase the size of the helium core is reduced by a deep second dredge-up, after which the core becomes degenerate and thermal pulses develop. In the $16.0 M_{\odot}$ case, convective core H- and He-burning is followed by core C-burning, and no 2nd dredge-up occurs. Ne ignites hydrostatically, and subsequent burning will lead to the formation of an iron core.

In accord with previous work (Ritossa et al. 1996; Iben et al. 1997; Garcia-Berro et al. 1997; Ritossa et al. 1999; Siess 2006), the second dredge-up reduces the helium core mass to values below the Chandrasekhar mass in our EVOL and STERN models. This leads to a clear definition of the upper mass limit of SAGB stars, as the critical mass between the occurrence and non-occurrence of the second dredge-up. For initial masses lower than this critical mass, Ne ignition is always avoided, while for initial masses higher than the critical mass the helium core mass is so large ($\sim 2.8 M_{\odot}$) that Ne always ignites. Our KEPLER models show a more complicated behavior: some show a second dredge-up depth which leaves helium cores with masses in between $1.4 M_{\odot}$ and $2.8 M_{\odot}$. However, those with post-dredge-up helium cores above the Chandrasekhar limit all ignite core Ne burning. We conclude that a second dredge-up down to the Chandrasekhar mass is required for an ECSN to occur, which thus defines our upper SAGB mass limit. This is also in line with the recent results of Eldridge & Tout (2004a), who do indeed find Ne shell flashes in some of their most massive models undergoing the second dredge-up; however the dredge-up does proceed to the Chandrasekhar mass, and the suggested fate of these models is that of an ECSN.

Figure 2 shows the helium core masses obtained in our detailed stellar evolution models. While the core mass after the 2nd dredge-up increases with initial mass for models computed with all three codes, differences arise with respect to the critical mass for second dredge-up. KEPLER and EVOL have similar final core masses, however they differ slightly with respect to the maximum core masses. These differences are related to the treatment of convection and overshooting. STERN uses the Ledoux-criterion for determining the convective boundaries, which naturally gives rise to smaller cores than the Schwarzschild-criterion. In these models no rotation was included, which – if included – would give significantly larger cores, due to rotationally induced mixing during the hydrogen and helium burning phases (Heger et al.

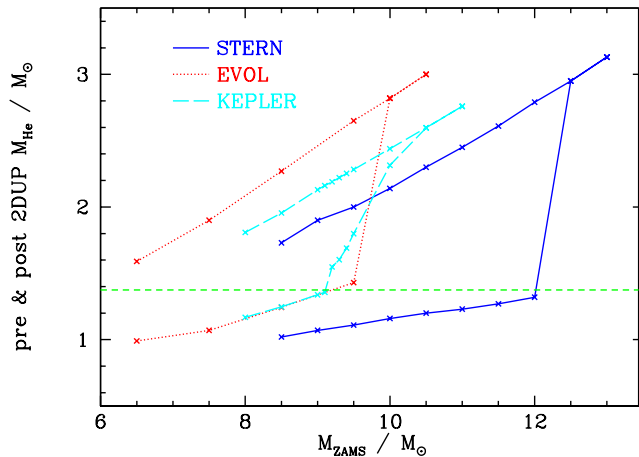


FIG. 2.— Helium core masses for stars of various initial masses, as obtained using different stellar evolution codes (solid line: STERN, dashed line: KEPLER, dotted line: EVOL). The upper part of the line shows the maximum size of the helium core, prior to the second dredge-up. The lower part shows the size of the helium core just after the completion of the second dredge-up and prior to the onset of the TP-AGB. The light dashed horizontal line gives the lower limit for the final helium core mass for which the star may experience an electron-capture supernova.

2000).

Using EVOL and KEPLER we find the transition between stars with and without a deep second dredge up at $\sim 9.25 M_{\odot}$. On the other hand, using STERN we find that stars more massive than $12 M_{\odot}$ do not experience a deep second dredge-up. The models in the mass range between $12 M_{\odot}$ and $12.5 M_{\odot}$ show a convective shell that develops on top of the helium burning layer (the so called dredge-out, c.f. Ritossa et al. 1999) which connects through a semiconvective layer with the bottom of the hydrogen-rich convective envelope. We find that protons are mixed into this hot layer and burn quickly. For a proper treatment of this interaction a scheme that solves the burning and mixing simultaneously is needed to follow the subsequent evolution of these stars. Since STERN is not equipped with such a scheme but calculates burning and mixing separately, we followed the subsequent evolution with very small timesteps until the code was not able to calculate further. Therefore, it remains unclear whether this semiconvective layer dissolves and on what time scale. If it would, the helium core masses would be reduced to just below the Chandrasekhar mass. If the semiconvective layer remains for the rest of the evolution of the star, it would allow Ne to ignite in the core and eventually lead to Fe-core collapse supernova. This renders the upper mass limit for SAGB stars according to the STERN models somewhat ambiguous in the range $12...12.5 M_{\odot}$.

In the EVOL models, the convective core overshooting was calibrated by the observed width of the main sequence. However, stars rotate, and the STERN code usually takes this into account. The effect of rotation also widens the main-sequence and in this way STERN models with rotation can reproduce the observed main-sequence width as well (Heger & Langer 2000). In this study we compute non-rotating models with STERN, in order to avoid the complex question of how rotational mixing affects SAGB properties. As a drawback, the initial mass range for SAGB stars found with STERN

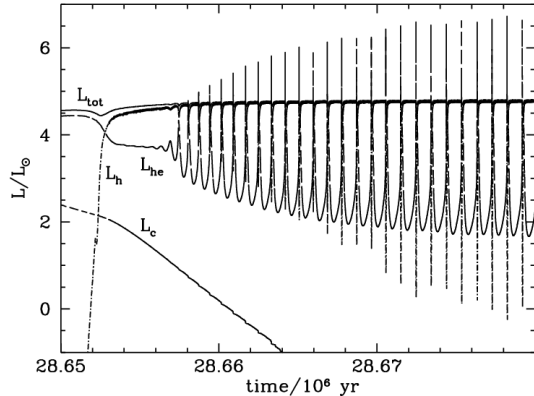


FIG. 3.— Nuclear burning luminosity contributions and total luminosity as a function of time at the onset of the thermal pulse phase for a $9M_{\odot}$ star calculated with STERN. At the time of second dredge-up hot-bottom burning starts, shown in the figure as a steep rise of the hydrogen luminosity.

is offset compared to the EVOL/KEPLER models by $\approx 2.75M_{\odot}$. Since the non-rotating STERN models do not reproduce the well-established main-sequence width, we prefer here the results of the EVOL/KEPLER models to derive the initial mass range for SAGB stars. Based on those, the upper mass limit for SAGB stars – and thus electron capture supernovae – is about $9.25M_{\odot}$ (Figure 2). Without knowledge about the subsequent phase – the thermally pulsing SAGB phase – we can only say that the lower limit for electron capture supernovae is $7.5M_{\odot}$, since stars with a lower mass do not ignite carbon.

4. THE TP-SAGB STELLAR EVOLUTION MODELS

4.1. Thermal Pulses and Hot Bottom Burning

Double shell burning of H and He on degenerate cores leads to periodic thermonuclear instabilities. These He-shell flashes or thermal pulses are an important site for nucleosynthesis in AGB stars, and cause mixing of the intershell region and — by way of the third dredge-up — mixing of processed material to the surface (Iben & Renzini 1983; Busso et al. 1999; Herwig 2005). Thermal pulses of SAGB stars are similar to thermal pulses of CO-core AGB stars (Ritossa et al. 1996). In order to obtain quantitative information on these SAGB thermal pulse cycles, we calculate such model sequences for several initial masses (Table 1).

As in massive AGB stars, most of the luminosity is produced by hot-bottom burning. During hot-bottom burning, hydrogen is transported convectively into the H-shell, and H-burning ashes are transported out of the shell into the envelope. In the more massive SAGB stars this hot-bottom burning starts immediately after the completion of the second dredge-up, and can proceed at very high temperatures. In our STERN models we obtain values of $1.0 \times 10^8\text{K}$ ($10M_{\odot}$ with $M_c = 1.16M_{\odot}$ after 30 thermal pulses) and $1.1 \times 10^8\text{K}$ ($11.5M_{\odot}$ with $M_c = 1.27M_{\odot}$ already at the first thermal pulse). The EVOL models show a similar trend with the $9.0M_{\odot}$ model (E0099) reaching temperatures at the bottom of the convective envelope of $1.13 \times 10^8\text{K}$ after the 12th pulse.

Hot-bottom burning could be stronger (or weaker) than in our calculations, e.g. due to convective overshoot-

ing at the bottom of the convective envelope, or due to a larger (or smaller) convective efficiency than assumed in most MLT based stellar evolution calculations. In that case, the accretion of He on the core may be so much reduced that the core does not or only very slowly grow. We have performed some test calculations with enhanced convective extra mixing during the hot-bottom phase. These tests show so far a stationary H-shell, which slowly processes its envelope, and no core growth, which results probably in a massive ONE white dwarf. Whether this theoretical possibility is occurring in real stars is not clear because the physics of a convective boundary inside the H-shell is poorly known.

SAGB stars show a He-peak luminosity during thermal pulses of around $\log L/L_{\odot} \sim 6$, which is significantly lower than obtained in massive AGB stars which reach luminosities up to $\log L/L_{\odot} \sim 8$. This may explain why the third dredge-up is less efficient in terms of the dredge-up parameter λ (see Sect. 4.2).

Extending the trend seen from low-mass to massive AGB stars, SAGB stars have smaller intershell masses (in the STERN $9M_{\odot}$ model of $7 \times 10^{-4}M_{\odot}$ at a core mass of $1.06M_{\odot}$), and the interpulse time is also lower, ranging from 50 yr for the $11.5M_{\odot}$ SAGB star with core mass of $1.27M_{\odot}$ to 1000 yr for a SAGB star with a mass of $9.0M_{\odot}$.

4.2. Efficiency of the 3rd dredge-up

The growth of the core during the TP-SAGB may be decreased by the dredge-up of material after a thermal pulse. The efficiency of the dredge-up (DUP) is expressed through the dredge-up parameter $\lambda = \Delta M_{\text{H}}/\Delta M_{\text{DUP}}$, where ΔM_{H} is the core mass increase due to H-burning during the interpulse phase, and ΔM_{DUP} is the mass that is dredged up by the convective envelope.

In the models calculated with STERN we did not observe any dredge-up. This result is consistent with results for non-rotating low mass AGB-stars (Siess et al. 2004) from the same code which are also calculated using the Ledoux-criterion for convection. Ritossa et al. (1996) and Siess & Pumo (2006) find a similar result. The recent models of Doherty & Lattanzio (2006) find very efficient dredge-up, e.g. $\lambda \approx 0.7$ for a $9.5M_{\odot}$ model. Observations clearly require a 3rd dredge-up in low-mass and massive AGB stars, since we see its result in terms of carbon and s-process enrichment in real AGB stars. However, the efficiency of the 3rd dredge-up in massive and SAGB stars is not constrained observationally, partly probably because of the high dilution factor in the massive envelope.

In order to get an idea about the efficiency of the 3rd dredge-up in super AGB stars and the robustness of our and previous results, we studied the behavior of the thermal pulses also with the EVOL code. We calculated a $9M_{\odot}$ model (E0099) until the 12th pulse. This model was computed with a four times smaller factor for the overshooting than the other EVOL models ($f_{\text{over}} = 0.004$) until the TP-AGB. This gives the star a smaller core than the regular models. On the TP-AGB a value of $f_{\text{over}} = 0.008$ was used. The first thermal pulse starts after the completion of the second dredge-up, when the bottom of the convective envelope is at $m_r = 1.17M_{\odot}$. The surface luminosity after 12 pulses is $\log L/L_{\odot} = 5.07$, the maximum helium luminosity dur-

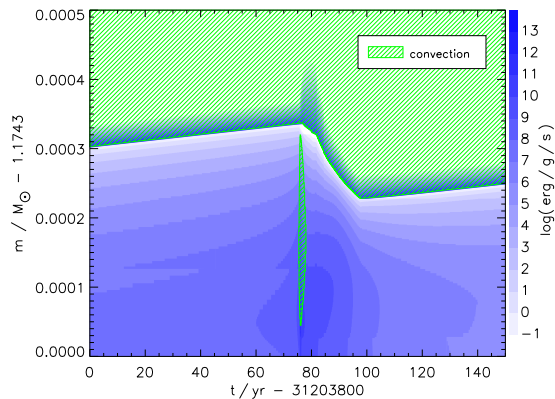


FIG. 4.— Evolution of the SAGB He-shell flash during the 12th pulse computed with the EVOL code (E0099). The dredge-up efficiency equals $\lambda = 0.5$.

ing the 12th pulse $\log L_{\text{He}}/L_{\odot} = 6.17$, and the duration of the interpulse period is ~ 500 yr.

After the eighth pulse, the ensuing mixing has the characteristics of a ‘hot’ dredge-up, first described for massive low-metallicity AGB stars by Herwig (2004a) and also found by Chieffi et al. (2001) for $Z = 0$ models. Any small amount of mixing of protons into the hot ^{12}C -rich layers — performed here by diffusive exponential overshooting — leads to violent H-burning which increases the convective instability. Like a flame, this corrosive hydrogen burning enforces the penetration of the convective envelope into the intershell (see Fig. 4). For this situation, we find efficient dredge-up ($\lambda \sim 0.5$), i.e. half of the interpulse core growth is dredged up, reducing the average pulse cycle core growth rate. Unfortunately the hot dredge-up phenomenon adds another source of uncertainty to dredge-up predictions as the dredge-up efficiency is extremely sensitive to the overshooting or extra-mixing efficiency at the bottom of the convective boundary.

5. THE SAGB POPULATION SYNTHESIS MODEL

Mass loss and the dredge-up are the two most important but also most uncertain processes that determine the final evolution of SAGB stars. Here we employ a simplified synthetic model that allows us to estimate the effect of different assumptions concerning these two processes on the initial mass range for ECSNe.

5.1. A simple estimate

We start with a simple back-of-the-envelope estimate: Stars that have, after carbon burning, a helium core mass larger than the Chandrasekhar mass (M_{Ch}) explode as CCSN. The Chandrasekhar mass of a cold iron core is $M_{\text{Ch-eff}} = 1.375 M_{\odot}$ (Sugimoto & Nomoto 1980; Nomoto 1981). In order to form an ECSN, the core mass has to grow from the mass at the beginning of the TP-AGB, $M_c(2DUP)$, to the Chandrasekhar mass by

$$\Delta M_c = M_{\text{Ch}} - M_c(2DUP). \quad (1)$$

This value depends strongly on the initial mass as Figure 5 shows.

Whether the core is able to grow by this amount depends only on the mass of the envelope, the core growth rate and the mass loss rate. Given these quantities, $\Delta M_{c,\text{max}}$ is the maximum mass that the core can grow.

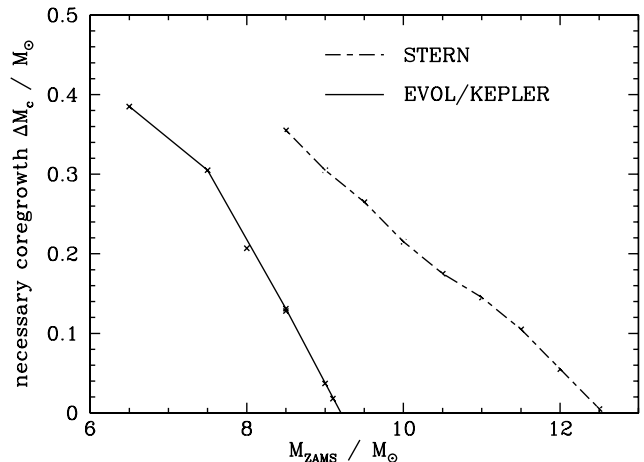


FIG. 5.— Mass ΔM_c by which the core needs to grow during the TP-AGB in order to reach the Chandrasekhar mass, as function of the initial mass. The upper boundary is given by stars that do not have a second dredge-up, so their cores are larger than the Chandrasekhar mass.

The core growth rate due to nuclear burning is dM_c/dt . Due to the 3rd dredge-up, the value for the core growth rate can decrease. We correct for this by introducing a factor $1 - \lambda$. The timescale on which the envelope of the star will be lost is

$$\tau_{\text{env}} = \frac{M_{\text{env}}}{dM/dt_{\text{env}}}, \quad (2)$$

and multiplied by the core growth rate this gives the maximum value that the core can grow. This gives an approximate relation for the growth of the core during the TP-SAGB phase

$$\Delta M_{c,\text{max}} = \frac{M_{\text{env}}}{dM/dt_{\text{env}}} \times (1 - \lambda) dM_c/dt. \quad (3)$$

For a typical, but constant, core growth rate of $\dot{M}_c = 5 \cdot 10^{-7} M_{\odot} \text{yr}^{-1}$, and an envelope mass of $M_{\text{env}} = 10 M_{\odot}$, Fig. 6 shows $\Delta M_{c,\text{max}}$ as a function of the mass loss rate, for two different values of λ (no dredge-up and $\lambda = 0.9$).

Figure 5 shows that in order to have an initial mass range for ECSN of, for example, $1 M_{\odot}$, the core growth during the SAGB phase must be of the order $0.1\text{--}0.2 M_{\odot}$. Figure 6 shows that if SAGB mass loss is larger than $\approx 10^{-4} M_{\odot}/\text{yr}$ such a core growth can not be achieved, even for inefficient 3rd dredge-up. For mass loss rates below $\approx 10^{-6} M_{\odot}/\text{yr}$, however, a core growth of a few $0.1 M_{\odot}$ is predicted even if $\lambda = 0.9$. Compared with the empirical mass loss rates derived by van Loon et al. (2005, hereafter L05, c.f. Table 2) it is clear that the initial mass range for ECSN is sensitive to the third dredge-up.

5.2. Synthetic SAGB evolution

A quantitative estimate of the initial mass range for ECSN can be obtained through a synthetic model for the TP-AGB phase, similar to that of Izzard et al. (2004, hereafter I04) for AGB stars, which is based on detailed AGB models from Karakas (Karakas et al. 2002). The extension to SAGB stars is made by fitting the TP-AGB evolution of detailed stellar evolution models (STERN) presented above, specifically over the mass range between 7 and $11.5 M_{\odot}$ in initial mass.

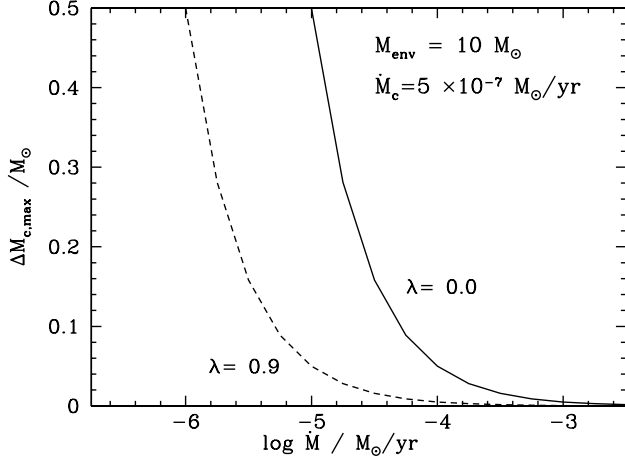


FIG. 6.— Expected core growth during the TP-SAGB (Eq. 3) as function of the mass loss rate, for two different dredge-up efficiencies λ as labeled. A constant mass loss rate, an envelope mass of $10 M_{\odot}$, and a constant core growth rate of $5 \times 10^{-7} M_{\odot}/\text{yr}^{-1}$ are assumed.

Based on the SAGB STERN evolution sequences with up to 30 thermal pulses, we derive fits for luminosity, radius, and Q-factor (see Sect. 5.2.3), as function of the core mass (M_c), the envelope mass (M_{env}) and as secondary parameters the metallicity (Z) and the envelope hydrogen abundance (X_{H}). Since the SAGB evolution models have entered into a quasi-steady state regime, these fits are good approximations for the subsequent evolution of SAGB stars during the TP-AGB in mass (total, core and envelope), luminosity and radius.

We then use these analytic expression as basis for our synthetic TP-SAGB model. As starting values for our synthetic SAGB calculation we use total mass, core mass, and envelope hydrogen abundance after the second dredge-up. First the luminosity is calculated from the initial core and envelope mass, then the radius is calculated, which is a function of the previously calculated luminosity and the envelope mass, and finally the core growth is calculated and integrated over a timestep dt . From these quantities, the effective temperature, mass loss rate, the resulting new mass of the envelope, and the new mass of the core are calculated. The new core mass and envelope mass are used as input for the next timestep.

In following subsections we describe the basic outline of our synthetic model (for details we refer to Izzard et al. 2004).

5.2.1. Luminosity and Radius

We follow I04 and model the luminosity with two terms, one which contains a core-mass–luminosity relation (CMLR) and one term due to hot-bottom burning. The total luminosity of the star can now be written as (cf. their Eq. 29)

$$L = f_d(f_t L_{\text{CMLR}} + L_{\text{env}}) L_{\odot}, \quad (4)$$

where L_{CMLR} is the core mass-luminosity relation given by

$$L_{\text{CMLR}} = 3.7311 \cdot 10^4 \times \max[(M_c/M_{\odot} - 0.52629)(2.7812 - M_c/M_{\odot}), 1.2(M_c/M_{\odot} - 0.48)] \quad (5)$$

if the core mass at the first thermal pulse, $M_{c,1\text{TP}}$ is $\geq 0.58 M_{\odot}$.

L_{env} is the contribution due to hot-bottom burning (e.g., I04:32),

$$L_{\text{env}} = 1.50 \cdot 10^4 \left(\frac{M_{\text{env}}}{M_{\odot}}\right)^{1.3} \left[1 + 0.75 \left(1 - \frac{Z}{0.02}\right)\right] \times \max\left[\left(\frac{M_c}{M_{\odot}} + \frac{1}{2} \frac{\Delta M_{c,\text{nodup}}}{M_{\odot}} - 0.75\right)^2, 0\right]. \quad (6)$$

M_c is the core mass, M_{env} is the envelope mass. $\Delta M_{c,\text{nodup}}$ is the change in core mass without third dredge-up and is defined by $\Delta M_{c,\text{nodup}} = M_{c,\text{nodup}} - M_{c,1\text{TP}}$ with $M_{c,\text{nodup}}$ the core mass as if there was no third dredge-up and $M_{c,1\text{TP}}$ the core mass at the first thermal pulse. Z is the metallicity. Note that we use a lower exponent than I04 in the contribution of the envelope mass, i.e. 1.3 instead of 2, which resulted in good fits for models between 7 and $11.5 M_{\odot}$.

The function

$$f_t = \min\left[\left(\frac{\Delta M_{c,\text{nodup}}/M_{\odot}}{0.04}\right)^{0.2}, 1.0\right] \quad (7)$$

accounts for the steep rise in luminosity at the beginning of the TP-AGB. The function

$$f_d = 1 - 0.2180 \exp[-11.613(M_c/M_{\odot} - 0.56189)] \quad (8)$$

corrects for the short timescale dips in the luminosity during the thermal pulse cycle.

For the fit to the radius we use an expression of the same form as given by I04, but with coefficients adjusted to the STERN models:

$$\log(f_r R) = -0.26 + 0.75 \log(L/L_{\odot}) - 0.41 \log(M_{\text{env}}/M_{\odot}) \quad (9)$$

with

$$f_r = 0.09 \log(M_{\text{env}}/M_{\text{env},0}) \quad (10)$$

a factor that accounts for the removal of the envelope, where $M_{\text{env},0}$ is the mass of the envelope at the first thermal pulse. This correction factor is determined by a fit to a $9 M_{\odot}$ model to which an extreme mass loss rate of $10^{-3} M_{\odot}/\text{yr}$ was applied. For envelope masses below $M_{\text{env}} = 2 M_{\odot}$ the fit predicts too large radii and it is not valid for temperatures below 2500 K as calculated from R and L .

5.2.2. Third Dredge-up

For the dependence of the third dredge-up on the initial mass we use the data from Karakas et al. (2002). Our own EVOL SAGB models, however, show smaller dredge-up ($\lambda = 0.5$ for $M_{\text{ini}} = 9 M_{\odot}$) than the extrapolation of the Karakas et al. (2002) data (Figure 7). We therefore extend the fit to higher masses with a relation that reflects our own data at $M_{\text{ini}} = 9 M_{\odot}$. To simulate a situation with no dredge-up, we also include in our synthetic code an option to set $\lambda = 0$.

5.2.3. Core growth and hot-bottom burning

The growth rate of the He core in the inter-pulse phase is given by

$$\frac{dM_c}{dt} = Q \times L \quad (11)$$

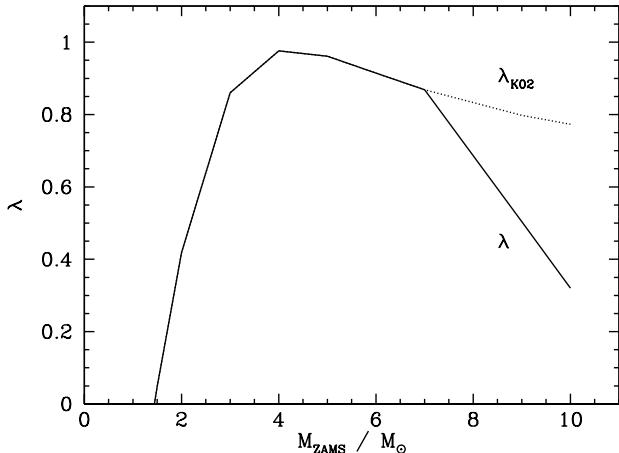


FIG. 7.— Dredge-up efficiency as a function of initial mass. The dotted line extrapolates the data by Karakas et al. (2002), while the solid line gives the modification based on our SAGB dredge-up stellar evolution sequence.

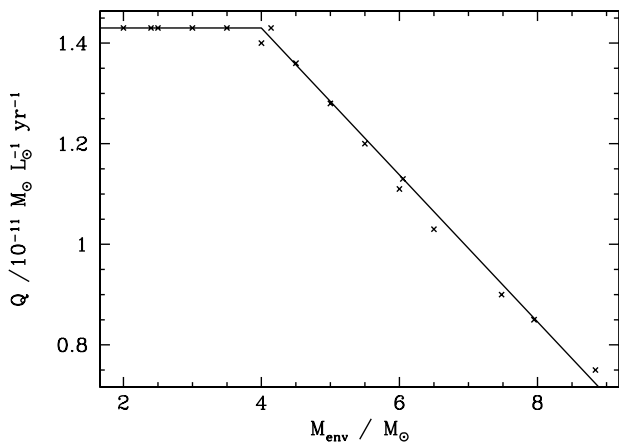


FIG. 8.— Ashes accreted on core per unit stellar energy release (Q) as a function of the mass of the envelope. For envelopes less massive than of $4 M_{\odot}$ there is no hot-bottom burning.

where L is the total luminosity of the star, and Q gives the mass of nuclear ashes accreted onto the core per energy released by the star. Q depends on several model properties, especially on the hot-bottom burning efficiency, and less on the chemical composition of the envelope. For massive AGB and SAGB stars its strength depends on the envelope mass. If the hot-bottom burning is efficient, Q can be small (see discussion in § 4.1), and the core may not significantly grow at all. Fig. 8 shows the decrease of Q with increasing envelope mass. We parameterize Q as

$$Q = \min\left[1.43 \times 10^{-11}, 1.40 \times 10^{-11} + \frac{4.166 \times 10^{-12}}{X_{\text{H}}} - 1.5 \times 10^{-12} \frac{M_{\text{env}}}{M_{\odot}}\right]. \quad (12)$$

This parameterization is in reasonable agreement with I04 who set Q to $1.585 \times 10^{-11} M_{\odot} L_{\odot}^{-1} \text{yr}^{-1}$, Hurley et al. (2000) who found $1.27 \times 10^{-11} M_{\odot} L_{\odot}^{-1} \text{yr}^{-1}$, and $1.02 \times 10^{-11} M_{\odot} L_{\odot}^{-1} \text{yr}^{-1}$ in Wagenhuber & Groenewegen (1998).

TABLE 2
MASS LOSS RATES FOR SAGB STARS WITH A TYPICAL VALUE FOR THE LUMINOSITY OF $\log L/L_{\odot} = 5$ AND AN EFFECTIVE TEMPERATURE OF $T_{\text{eff}} = 3000\text{K}$.

	Type	Rate
Reimers ($\eta = 1$)	Red Giants	$\sim 5 \cdot 10^{-6} M_{\odot}/\text{yr}$
Reimers ($\eta = 4$)	Red Giants	$\sim 2 \cdot 10^{-5} M_{\odot}/\text{yr}$
Schröder & Cuntz	Super Giants	$\sim 1 \cdot 10^{-5} M_{\odot}/\text{yr}$
van Loon	AGB/RSG	$\sim 3 \cdot 10^{-5} M_{\odot}/\text{yr}$
Blöcker	AGB	$\sim 6 \cdot 10^{-3} M_{\odot}/\text{yr}$
Vassiliadis & Wood	AGB	$\sim 4 \cdot 10^{-5} M_{\odot}/\text{yr}$

5.2.4. Mass loss

As discussed in § 5.1 the mass loss of SAGB stars is the other important factor to determine the initial mass range of ECSN. SAGB stars are O-rich (because of hot-bottom burning), and have stellar parameters around $\log T_{\text{eff}} = 3.5$ and $\log L/L_{\odot} = 5$ at solar metallicity. It is not clear what the dominant mass loss mechanism for these stars is. Are they cool enough to develop dust-driven winds or is mass loss simply driven by radiation pressure?

Table 2 shows a compilation of observational and theoretical mass loss rates, for a combination of typical SAGB parameters. Note, however, that these rates are not constant over time, and that the variation itself during the AGB phase is important for the final outcome. We preferentially use the observed mass loss rates for massive AGB stars and red supergiants by van Loon et al. (2005, L05). If dust-formation does not play an important role, then the Reimers mass loss rate (Reimers 1975), may be applicable. It is derived from observations of RGB stars with a small range in temperatures and radii, however, Schröder & Cuntz (2005) have revised the Reimers rate. For the more massive RSG stars their new approach, which also includes surface gravity, gives about three times larger mass loss than the Reimers formula. This places it, for given temperature and luminosity (c.f. Table 2), within a factor of 2 of the observational mass loss determination by L05. The mass loss formula by Vassiliadis & Wood (1993) (hereafter VW93), which is often used for AGB star evolution calculations, is also close to the observational value. The AGB mass loss formulated by Blöcker (1995), and based on the hydrodynamic wind models by Bowen (1988) has a higher luminosity exponent, and gives very high mass loss rates for SAGB stars. From our first estimate in Sect. 5.1 it is clear that with the Bloecker mass loss SAGB stars would never explode as ECSN.

6. RESULTS

We perform a series of synthetic calculations, with two assumptions on third dredge-up and three assumptions on mass loss. For dredge-up we assume either the parameterization of § 5.2.2 or $\lambda = 0$. For mass loss, we consider the cases Reimers, L05, and VW93 (§ 5.2.4).

6.1. Initial mass range for ECSN

The resulting initial mass ranges for ECSN are illustrated in Figure 9 for the case with parameterized λ , and in Figure 10 for $\lambda = 0$. Stars that end their evolution as white dwarf, i.e. below the Chandrasekhar mass, do not explode as ECSNe. With the parameterized prescription for the third dredge-up, the width of the initial mass

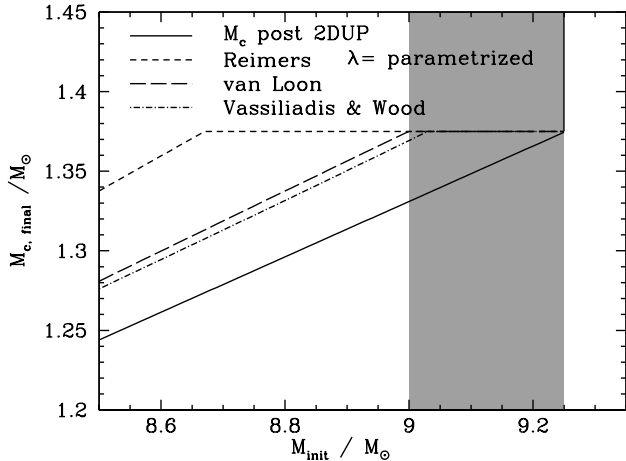


FIG. 9.— Final core mass as a function of initial mass based on synthetic SAGB calculations. The solid line indicates the post second dredge-up core mass, the short dashed line indicates the final core mass using the Reimers mass loss rate ($\eta = 4$), the dashed line using the L05 mass loss rate, and the dash-dotted line using the VW93 mass loss rate. The shaded region indicates the initial mass range for ECSNe for the L05 mass loss rate.

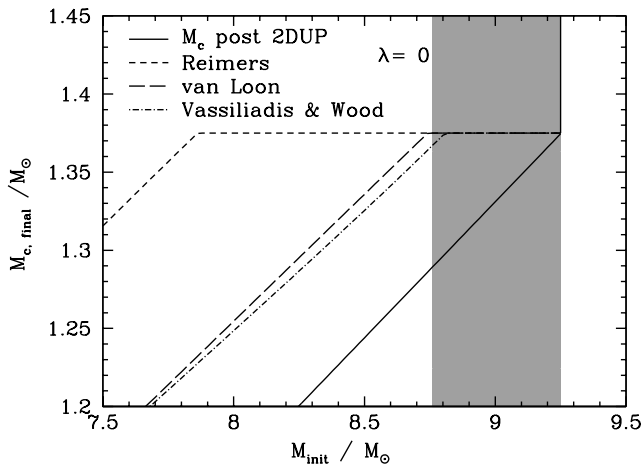


FIG. 10.— Same as Figure 9 but for calculations assuming no dredge-up. Note different x-axis scale.

window for which ECSN occurs is between $0.25 M_{\odot}$ and $0.65 M_{\odot}$, depending on the assumed mass loss rate. The mass loss prescriptions of L05 and of VW93 give an initial mass window of $0.20 - 0.25 M_{\odot}$. With zero dredge-up, the core grows at the maximum possible rate. The width of the initial mass window for ECSN is between $1.4 M_{\odot}$ for the Reimers mass loss rate and $0.45 - 0.5 M_{\odot}$ for the VW93 and L05 mass loss rates.

6.2. ECSN fraction

Based on the inferred mass ranges from the synthetic model, we determine the ratio of the number of ECSNe to the total number of SNe. Table 3 gives an overview of the results for the cases of parameterized dredge-up and without dredge-up ($\lambda = 0$), assuming the Salpeter IMF. The value of λ has a strong influence on the predicted fractions. With the parameterized dredge-up and the VW93 or L05 mass loss rates the ECSN fraction of all supernovae is about 3.5%. With the Reimers mass loss rate 8% of all supernovae are ECSN. The largest ECSN

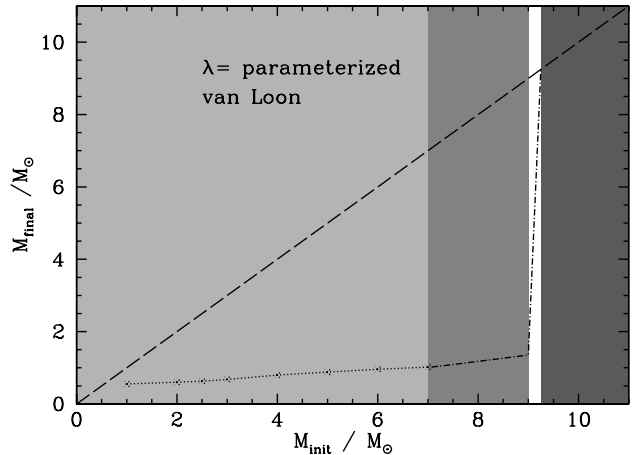


FIG. 11.— Final mass of the remnant as a function of the initial mass. Remnant regimes are shaded as *light grey*: CO-white dwarf; *grey*: ONe white dwarf; *white*: ECSN; *dark grey*: CCSN. The final mass is either the WD mass or the stellar mass at the time of SN explosion. The dashed line indicates the line of initial mass equal final mass.

fraction of 20% is obtained without dredge-up and using the Reimers mass loss rate.

6.3. Final mass and SN properties

Figure 11 shows the initial-final mass relation for the mass range from $1.0 M_{\odot}$ to $14 M_{\odot}$ using the parameterized dredge-up prescription and the L05 mass loss rate. For ECSNe, we find a large spread in progenitor and envelope masses. The least massive SAGB SN progenitors lose almost their entire envelope, growing the core just barely enough to still make an electron capture supernovae before the envelope is lost. The most massive SAGB SN progenitors, on the other hand, undergo very little TP-AGB mass loss before they explode, and contain a massive hydrogen-rich envelope at that time.

This diversity is a natural consequence of the competition between core growth and mass loss during the SAGB stage, and thus independent of the choice of mass loss rate and dredge-up parametrisation. The expected envelope mass range, from almost zero to about $8 M_{\odot}$ (Fig. 12), implies a diversity of supernova light curves of ECSNe, which may range from light curves of so called Type IIb and Type IIL supernovae to those of typical Type IIP supernovae (Falk & Arnett 1977; Young 2004).

However, ECSNe may show three properties which might allow to distinguish them from ordinary Type II supernovae. First, they might produce low-energy explosions (Kitaura et al. 2006) and possibly low neutron star kicks (Podsiadlowski et al. 2004). A consequence of the low explosion energy may be a small nickel mass produced by the explosion, and thus a low luminosity of the tail of the light curve which is produced by the decay of ^{56}Ni and ^{56}Co (Kitaura et al. 2006). The Type IIP SN 1997D may provide an example (Chugai & Utrobin 2000). Second, however, the enormous mass loss rate of the supernova progenitor (Fig. 14) star may produce clear signatures of a supernova-circumstellar medium interaction in the supernova light. Such signatures are in particular exceptionally a bright and long-lasting light curve (Sollerman et al. 2001), and narrow hydro-

TABLE 3

INITIAL MASS LIMITS FOR ECSN AND RATIO OF ECSN TO SN AS A FUNCTION OF THE DREDGE-UP EFFICIENCY AND MASS LOSS PRESCRIPTION.

	$\lambda = \text{parameterized}$			$\lambda = 0$		
	M_{low}/M_{\odot}	$M_{\text{high}}/M_{\odot}$	% EC	M_{low}/M_{\odot}	$M_{\text{high}}/M_{\odot}$	% EC
Reimers ($\eta = 4$)	8.67	9.25	8.4	7.86	9.25	19.7
VW93	9.03	9.25	3.2	8.82	9.25	6.2
L05	9.00	9.25	3.6	8.76	9.25	7.1

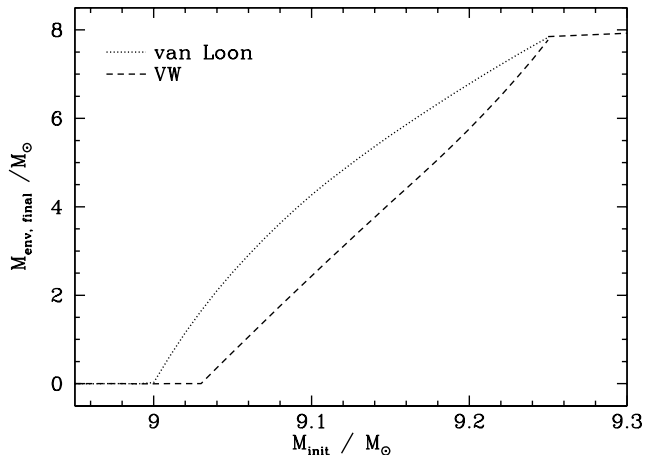


FIG. 12.— Mass of the envelope just prior to the explosion as function of the initial mass for two mass loss rates.

gen emission lines superimposed to a typical SN II spectrum (Pastorello et al. 2002). Third, ECSN progenitors are extremely bright, with luminosities of the order of $10^5 L_{\odot}$ (Fig. 13). Thus, progenitor identifications on pre-explosion images (Maund & Smartt 2005; Hendry et al. 2006) might be able to identify ECSNe. They may be distinguished from very massive ($> 20 M_{\odot}$) progenitors of similar luminosity by their much cooler effective temperatures ($< 3000\text{K}$ for ECSN progenitors versus $\sim 3400\text{K}$ for CCSN progenitors).

6.4. The reference model, examples

As shown above, the results of our synthetic SAGB calculations employing the VW93 and the L05 mass loss prescriptions are rather similar. Since it is unclear whether the Reimers mass loss rate is really applicable, and as the L05 mass loss rate relies on very recent observations, we adopt the latter as the fiducial mass loss prescription for our synthetic SAGB modeling. Concerning the third dredge-up efficiency, we adopt the mass dependant formulation shown in Fig. 7 as our reference efficiency. These assumptions define our reference model for the synthetic SAGB evolution.

In the following, we discuss some explicit examples to illustrate the TP-SAGB evolution, and to further motivate the choice of our reference model and analyse its uncertainty. The first example is a star with an initial mass of $9.1 M_{\odot}$, with a He-core mass at the end of the second dredge-up of $1.348 M_{\odot}$.

During the evolution on the TP-SAGB the luminosity first increases from $\log L/L_{\odot} = 4.9$ to $\log L/L_{\odot} = 5.02$, and then drops slightly due to decreasing envelope mass which decreases the efficiency of hot-bottom burning. As a result, the inter-pulse core growth rate increases from

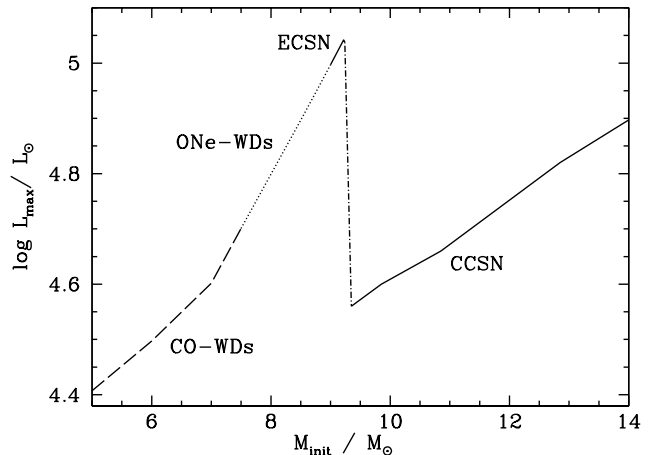
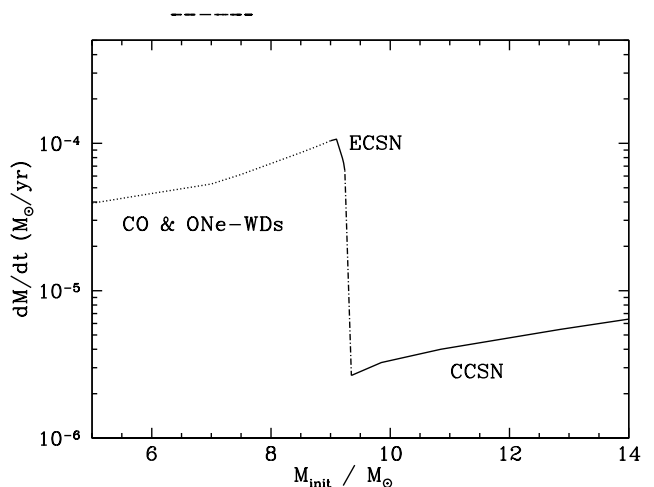
FIG. 13.— Maximum luminosity as function of the initial mass at the end of the evolution. Progenitors of CO white dwarfs reach luminosities up to $\log L/L_{\odot} \sim 4.6$, progenitors of ONe white dwarfs reach luminosities up to $\log L/L_{\odot} \sim 5$. Progenitors of ECSN are the most luminous, with $\log L/L_{\odot} \geq 5$, while progenitors of the least massive CCSN have pre-explosion luminosities of $\log L/L_{\odot} \sim 4.6$ 

FIG. 14.— Mass loss rates according to L05 as function of initial mass, for the models shown in Fig. 13.

$3 \times 10^{-7} M_{\odot}/\text{yr}$ to $1.5 \times 10^{-6} M_{\odot}/\text{yr}$, but the effective core growth is significant lower (by about factor 0.5) due to the effect of dredge-up. The mass loss rate increases from $3 \times 10^{-5} M_{\odot}/\text{yr}$ to $1 \times 10^{-4} M_{\odot}/\text{yr}$ (Fig. 15). In this model the SAGB ends after $\sim 4.4 \times 10^4$ yr when the core reaches its Chandrasekhar mass. The remaining envelope has a mass of $4.27 M_{\odot}$.

For a 10% larger dredge-up efficiency the SAGB time increases to $\sim 4.8 \times 10^4$ yr, and the remaining envelope

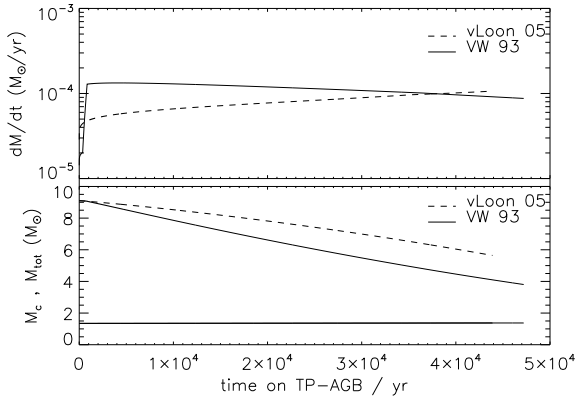


FIG. 15.— Synthetic AGB mass evolution for an initial mass of $9.1 M_{\odot}$. Upper panel: mass loss rate for two cases (L05 and VW93, § 5.2.4); the superwind regime in the VW93 mass loss prescription sets in at 1000yr right at the beginning of the AGB phase. Lower panel: evolution of the core and the total stellar mass.

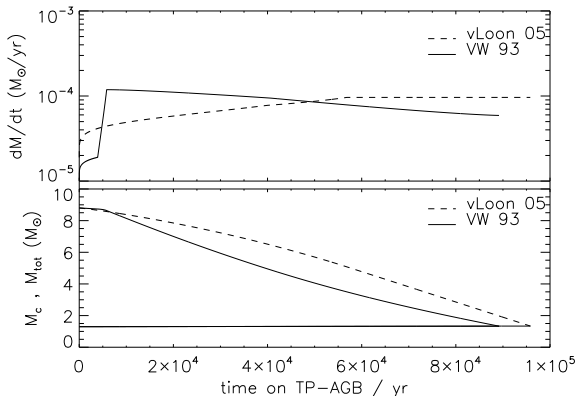


FIG. 16.— Similar to Figure 15 but for a $8.8 M_{\odot}$ star. The core does not reach the Chandrasekhar mass but loses its envelope and becomes a massive ONe white dwarf.

decreases to $3.82 M_{\odot}$. For a 10% smaller dredge-up efficiency the SAGB decreases to $\sim 4.0 \times 10^4$ yr, and the final envelope mass increases to $4.61 M_{\odot}$. For the case of no dredge-up the SAGB time is $\sim 2.4 \times 10^4$ yr and the final envelope mass is $6.1 M_{\odot}$.

Using the mass loss prescription of VW93 and the parameterized dredge-up, the result is only different in the mass loss history, resulting in a smaller final mass. The main reason is that this mass loss prescription accounts for the superwind phase for TP-AGB stars, which gives a significantly different evolution of the envelope. The TP-AGB phase starts with low mass loss but makes a transition to the superwind phase after 1000 yr with mass loss rates around $1 \times 10^{-4} M_{\odot}/\text{yr}$, decreasing slowly due to the waning luminosity (Fig. 15, Upper Panel). After 4.7×10^4 yr, the core reaches its Chandrasekhar mass with a final envelope mass of $2.43 M_{\odot}$.

An initially $8.8 M_{\odot}$ star with the same mass loss and dredge-up (Fig. 16) becomes an ONe WD. The He-core mass at the beginning of the SAGB is $1.296 M_{\odot}$. During the SAGB evolution the luminosity increases to $\log L/L_{\odot} = 4.95$, then decreases due to mass loss. Assuming the L05 mass loss rate, the envelope is lost after $\sim 1 \times 10^5$ yr. The mass loss rate increases steadily during the TP-AGB phase, but as the star reaches a surface temperature of 2500K (Sect. 5.2) we assume a constant

mass loss rate of $\dot{M} = 1 \times 10^{-4} M_{\odot}/\text{yr}$ during the last phase of the evolution. This is consistent with the observations of L05 who find only one star with a higher mass loss rate. The remaining ONe core has a mass of $1.338 M_{\odot}$. Repeating this calculation with the mass loss rate of VW93 does not show large differences (Fig. 16).

7. CONCLUDING REMARKS

We show that both the lower initial mass for SAGB stars and the maximum initial mass for ECSNe sensitively depend on the assumptions for mixing during core H- and He-burning. EVOL models which include core overshooting, and which are consistent with the observed width of the main sequence, predict a smaller maximum initial mass for SAGB stars. Rotation would act similar to overshooting during the core burning phases. The STERN models include neither rotation nor overshooting, and the maximum initial mass for SAGB and ECSNe is larger by up to $2.5 M_{\odot}$. Equally important is the treatment of semiconvection during He-core burning.

On the other hand, the lower initial mass limit for ECSNe is determined by the stellar properties on the SAGB. Most important are the third dredge-up efficiency, the mass loss rate, and the hot-bottom burning efficiency and its dependence on the adopted convection theory for the envelope. In general, larger mass loss, larger dredge-up efficiency and large hot-bottom efficiency all decrease the initial mass range for ECSNe, or even suppress the ECSN channel. In order to increase the accuracy of the transition initial mass between ECSNe and CCSNe and of the lower mass limit for ECSNe, these classical issues of stellar evolution need to be improved specifically for the initial mass range of 6 to $12 M_{\odot}$.

We have discussed here the SAGB stars with C-ignition and formation of ONe cores as the most likely progenitors of an ECSN class of supernova. It is in principle possible that initially less massive stars that develop CO cores could increase their core size on the TP-AGB up to the Chandrasekhar mass resulting in a supernova explosion. Despite the uncertainties still involved we can rule out this possibility for solar metallicity. There are two main reasons that prevent these SN1.5a from occurring: First, the mass loss would have to be much lower than observed. Second, models predict that the third dredge-up is larger for massive AGB stars with initial mass between 4 and $7 M_{\odot}$ than for SAGB stars (Fig. 7; Karakas et al. 2002). This makes it even more unlikely for massive AGB stars to significantly grow their cores.

We did not take into account mass loss until the beginning of the thermally pulsing phase. If mass loss were applied during the main sequence and up to the TP-AGB, less than half a solar mass would have been lost (Siess 2006, their Table 5). This may shift the quoted initial masses to a slightly higher value.

We note that there is large disagreement between the different studies on the dredge-up efficiency in SAGB stars (Ritossa et al. 1996; Doherty & Lattanzio 2006; Siess & Pumo 2006). Whereas Ritossa et al. (1996) and Siess & Pumo (2006) find negligible amounts of dredge-up, Doherty & Lattanzio (2006) find very efficient dredge-up with $\lambda \sim 0.7$. This situation is similar to the divergent modeling results obtained in the past on the third dredge-up in low-mass AGB stars. For the low-mass regime there is now some consensus that

TABLE 4

FINAL CORE AND ENVELOPE MASSES FOR DIFFERENT INITIAL MASSES. THE FIRST THREE COLUMNS GIVE THE INITIAL CONDITIONS OF THE MODELS. MODELS MARKED WITH AN ASTERISK ARE CALCULATED UNTIL THE END OF THE SECOND DREDGE-UP WITH EVOL (TABLE ??), THE OTHER MODELS ARE INTERPOLATED ASSUMING A LINEAR RELATION BETWEEN THE INITIAL MASS AND THE CORE MASS AT THE END OF THE SECOND DREDGE-UP. THE FOURTH AND THE FIFTH COLUMN GIVE THE FINAL CORE AND ENVELOPE MASS FOR TWO DIFFERENT MASS LOSS PRESCRIPTIONS (§ 5.2.4) AND FOR A PARAMETERIZED DREDGE-UP EFFICIENCY (§ 5.2.2). THE SIXTH AND SEVENTH COLUMN GIVE THE FINAL CORE AND ENVELOPE MASS FOR A DREDGE-UP EFFICIENCY OF ZERO. IN CASE A COLUMN CONTAINS "WD" OR "NS", THE REMNANT IS RESPECTIVELY A WHITE DWARF OR A NEUTRON STAR. ALL MASSES ARE IN UNITS OF A SOLAR MASS.

initial conditions			final conditions param. λ				final conditions $\lambda = 0$			
M_{tot}	M_{c}	M_{env}	$L05$		$VW 93$		$L05$		$VW 93$	
			M_{c}	M_{env}	M_{c}	M_{env}	M_{c}	M_{env}	M_{c}	M_{env}
6.5000*	0.9900	5.5100	1.0039	WD	1.0060	WD	1.0816	WD	1.0887	WD
7.5000*	1.0700	6.4300	1.0886	WD	1.0903	WD	1.1734	WD	1.1739	WD
8.5000*	1.2440	7.2560	1.2809	WD	1.2761	WD	1.3358	WD	1.3255	WD
8.7500	1.2875	7.4625	1.3282	WD	1.3223	WD	NS	0.2075	1.3654	WD
8.8000	1.2962	7.5038	1.3376	WD	1.3316	WD	NS	1.3774	1.3736	WD
8.9000	1.3136	7.5864	1.3563	WD	1.3504	WD	NS	3.2631	NS	1.4514
9.0000	1.3310	7.6690	NS	0.0221	1.3693	WD	NS	4.7723	NS	3.0680
9.1000	1.3484	7.7516	NS	4.2672	NS	2.4311	NS	6.0628	NS	4.7208
9.2000	1.3658	7.8342	NS	6.7800	NS	5.7643	NS	7.2711	NS	6.6314
9.2500	1.3745	7.8755	NS	7.8321	NS	7.7731	NS	7.8481	NS	7.8138

most of the differences were related to different physical and numerical treatments of the convective boundaries. Possibly the same applies to the divergent results for SAGB stars. In our synthetic model we adopted a parameterized prescription (Fig. 7) that is based on state-of-the-art full stellar evolution calculations. To test the effect of dredge-up we also considered a case with no dredge-up. Clearly, the third dredge-up in SAGB stars needs to be studied in more detail. It is closely related to the mixing conditions at the bottom of the convective boundary. This is a hydrodynamic situation which requires multi-dimensional simulation which is complicated by the fact that for these extremely massive cores the dredge-up seems to be hot (Herwig 2004a), i.e., any small amount of H that could be mixed across the convective boundary will instantly burn violently with all the associated feedback on the evolution of the convective instability in that region. On the other hand, the amount of material that is dredged up from the He intershell will be very small, even with large values of λ , due to the thin intershell, and will therefore easily dilute in the envelope.

It is presently not known whether ECSNe from SAGB stars contribute to the r -process pattern in the universe. Explosions from stars in this mass range have been investigated as promising site for the astrophysical r -process (Wheeler et al. 1998; Sumiyoshi et al. 2001; Wanajo et al. 2003), based on the work of Hillebrandt et al. (1984) who exploded a One core

model from Nomoto (1984, 1987). Other groups were not able to confirm the r -process contribution due to the low entropy (e.g., Burrows & Lattimer 1985; Baron et al. 1987; Mayle & Wilson 1988; Bethe & Wilson 1985). Kitaura et al. (2006) ruled out this possibility based on updated physics and two different nuclear equations of state.

In any case, our study outlines that ECSNe from SAGB stars are likely to occur, if only at a level of a few percent of the Type II supernova rate in the local universe. However, at low metallicity, the key physical ingredients to the evolution of thermally pulsing SAGB stars may change. In particular, the stellar wind mass loss rate may be lower, which might open the ECSN channel appreciably, and may even allow Type 1.5 supernovae. This issue will be discussed in a forthcoming paper.

This work has been in part supported by the Netherlands Organization for Scientific Research (NWO) (AJP). AH and FH are supported under the auspices of the National Nuclear Security Administration of the U.S. Department of Energy at Los Alamos National Laboratory under Contract No. DE-AC52-06NA25396. This research was supported by the DOE Program for Scientific Discovery through Advanced Computing (SciDAC); DOE DE-FC02-01ER41176 and DOE DE-FC-02-06ER41438).

REFERENCES

- Baron, E., Cooperstein, J., & Kahana, S. 1987, *ApJ*, 320, 300
 Bethe, H. A. & Wilson, J. R. 1985, *ApJ*, 295, 14
 Blöcker, T. 1995, *A&A*, 297, 727
 Bowen, G. H. 1988, *ApJ*, 329, 299
 Burrows, A. & Lattimer, J. M. 1985, *ApJ*, 299, L19
 Busso, M., Gallino, R., & Wasserburg, G. J. 1999, *ARA&A*, 37, 239
 Chieffi, A., Domínguez, I., Limongi, M., & Straniero, O. 2001, *ApJ*, 554, 1159
 Chugai, N. N. & Utrobin, V. P. 2000, *A&A*, 354, 557
 Denissenkov, P. A. & Tout, C. A. 2003, *MNRAS*, 340, 722
 Doherty, C. L. & Lattanzio, J. C. 2006, *Memorie della Societa Astronomica Italiana*, 77, 828
 Eldridge, J. J. & Tout, C. A. 2004a, *Memorie della Societa Astronomica Italiana*, 75, 694
 —. 2004b, *MNRAS*, 353, 87
 Falk, S. W. & Arnett, W. D. 1977, *ApJS*, 33, 515
 Freytag, B., Ludwig, H.-G., & Steffen, M. 1996, *A&A*, 313, 497
 Frost, C. A., Cannon, R. C., Lattanzio, J. C., Wood, P. R., & Forestini, M. 1998, *A&A*, 332, L17
 Garcia-Berro, E., Ritossa, C., & Iben, I. J. 1997, *ApJ*, 485, 765
 Girardi, L., Bressan, A., Bertelli, G., & Chiosi, C. . 2000, *A&AS*, 141, 371
 Gutiérrez, J., Canal, R., & García-Berro, E. 2005, *A&A*, 435, 231
 Habing, H. J. 1996, *A&A Rev.*, 7, 97
 Hashimoto, M., Iwamoto, K., & Nomoto, K. 1993, *ApJ*, 414, L105
 Heger, A. & Langer, N. 2000, *ApJ*, 544, 1016

- Heger, A., Langer, N., & Woosley, S. E. 2000, *ApJ*, 528, 368
- Hendry, M. A., Smartt, S. J., Crockett, R. M., Maund, J. R., Gal-Yam, A., Moon, D.-S., Cenko, S. B. and Fox, D. W., Kudritzki, R. P., Benn, C. R., & Østensen, R. 2006, *MNRAS*, 369, 1303
- Herwig, F. 2000, *A&A*, 360, 952
- 2004a, *ApJ*, 605, 425
- 2004b, *ApJS*, 155, 651
- Herwig, F. 2005, *ARAA*, 34
- Herwig, F. & Austin, S. M. 2004, *ApJ Lett.*, 613, L73
- Herwig, F., Blöcker, T., Schönberner, D., & El Eid, M. F. 1997, *A&A*, 324, L81
- Herwig, F., Langer, N., & Lugaro, M. 2003, in *IAU Symposium*, 99
- Hillebrandt, W., Wolff, R. G., & Nomoto, K. 1984, *A&A*, 133, 175
- Hurley, J. R., Pols, O. R., & Tout, C. A. 2000, *MNRAS*, 315, 543
- Iben, I. & Renzini, A. 1983, *ARA&A*, 21, 271
- Iben, I. J., Ritossa, C., & Garcia-Berro, E. 1997, *ApJ*, 489, 772
- Iglesias, C. A. & Rogers, F. J. 1996, *ApJ*, 464, 943
- Izzard, R. G., Tout, C. A., Karakas, A. I., & Pols, O. R. 2004, *MNRAS*, 350, 407
- Karakas, A. I., Lattanzio, J. C., & Pols, O. R. 2002, *Publications of the Astronomical Society of Australia*, 19, 515
- Kitaura, F. S., Janka, H.-T., & Hillebrandt, W. 2006, *A&A*, 450, 345
- Langer, N. 1998, *A&A*, 329, 551
- Langer, N., Fricke, K. J., & Sugimoto, D. 1983, *A&A*, 126, 207+
- Langer, N., Heger, A., Wellstein, S., & Herwig, F. 1999, *A&A*, 346, L37
- Marigo, P., Bressan, A., & Chiosi, C. 1996, *A&A*, 313, 545
- Maund, J. R. & Smartt, S. J. 2005, *MNRAS*, 360, 288
- Mayle, R. & Wilson, J. R. 1988, *ApJ*, 334, 909
- Miyaji, S. & Nomoto, K. 1987, *ApJ*, 318, 307
- Miyaji, S., Nomoto, K., Yokoi, K., & Sugimoto, D. 1980, *PASJ*, 32, 303
- Nomoto, K. 1981, in *IAU Symp. 93: Fundamental Problems in the Theory of Stellar Evolution*, 295–314
- Nomoto, K. 1984, *ApJ*, 277, 791
- 1987, *ApJ*, 322, 206
- Pastorello, A., Turatto, M., Benetti, S., Cappella ro, E., Danziger, I. J., Mazzali, P. A., Patat, F., Filippenko, A. V., Schlegel, D. J., & Matheson, T. 2002, *MNRAS*, 333, 27
- Podsiadlowski, P., Langer, N., Poelarends, A. J. T., Rappaport, S., Heger, A., & Pfahl, E. 2004, *ApJ*, 612, 1044
- Reimers, D. 1975, *Memoires of the Societe Royale des Sciences de Liege*, 8, 369
- Renzini, A. & Voli, M. 1981, *A&A*, 94, 175
- Ritossa, C., Garcia-Berro, E., & Iben, I. J. 1996, *ApJ*, 460, 489
- Ritossa, C., Garcia-Berro, E., & Iben, I. J. 1999, *ApJ*, 515, 381
- Sackmann, I.-J. & Boothroyd, A. I. 1991, *ApJ*, 366, 529
- Schröder, K.-P. & Cuntz, M. 2005, *ApJ*, 630, L73
- Siess, L. 2006, *A&A*, 448, 717
- Siess, L., Goriely, S., & Langer, N. 2004, *A&A*, 415, 1089
- Siess, L. & Pumo, M. L. 2006, *Memorie della Societa Astronomica Italiana*, 77, 822
- Sollerman, J., Kozma, C., & Lundqvist, P. 2001, *A&A*, 366, 197
- Sugimoto, D. & Nomoto, K. 1980, *Space Science Reviews*, 25, 155
- Sumiyoshi, K., Terasawa, M., Mathews, G. J., Kajino, T., Yamada, S., & Suzuki, H. 2001, *ApJ*, 562, 880
- van Loon, J. T., Cioni, M.-R. L., Zijlstra, A. A., & Loup, C. 2005, *A&A*, 438, 273
- Vassiliadis, E. & Wood, P. 1993, *ApJ*, 413, 641
- Ventura, P., Castellani, M., & Straka, C. W. 2005, *A&A*, 440, 623
- Wagenhuber, J. & Groenewegen, M. A. T. 1998, *A&A*, 340, 183
- Wanajo, S., Tamamura, M., Itoh, N., Nomoto, K., Ishimaru, Y., Beers, T. C., & Nozawa, S. 2003, *ApJ*, 593, 968
- Weaver, T. A., Zimmerman, G. B., & Woosley, S. E. 1978, *ApJ*, 225, 1021
- Wheeler, J. C., Cowan, J. J., & Hillebrandt, W. 1998, *ApJ*, 493, L101
- Woosley, S. E., Heger, A., & Weaver, T. A. 2002, *Reviews of Modern Physics*, 74, 1015
- Yoon, S.-C., Langer, N., & van der Sluys, M. 2004, *A&A*, 425, 207
- Young, P. A., Meakin, C., Arnett, D., & Fryer, C. L. 2005, *ApJ Lett.*, 629, L101
- Young, T. R. 2004, *ApJ*, 617, 1233